

James H. Hanson¹ and Anthony R. Ingraffea²

Compression Loading Applied to Round Double Beam Fracture Specimens. II: Derivation of Geometry Factor

ABSTRACT: The round double beam loaded in eccentric compression has been shown to produce usable data when determining the fracture properties of materials with a relatively large characteristic length. In order to reduce these data, the geometry calibration factor must be known for the combination of specimen geometry and loading technique. Numerical simulations using the boundary element method have been used to determine the geometry calibration factor for a round double beam with a length to diameter ratio of 2:1 loaded in eccentric compression. The factor was determined by compliance calibration and direct calculation of stress intensities. Recognizing that laboratory test specimens will not have exactly the same geometry as the simulated specimen, geometry calibration factors have been determined for variations in the base geometry as well.

KEYWORDS: fracture toughness testing, round double beam specimen, eccentric compression loading, geometry calibration factor, compliance calibration, stress intensity factor, finite-element analysis

Introduction

The round double beam, RDB, is a cylindrical test specimen with a chevron notch developed by Barker [1]. The specimen is used in standards for measuring the fracture toughness of rock [2], cemented carbides (ASTM B 771, Standard Test Method for Short Rod Fracture Toughness of Cemented Carbides), and metals (ASTM E 1304, Standard Test Method for Plane-Strain (Chevron-Notch) Fracture Toughness of Metallic Materials). All of these standards load the RDB in tension or wedging. The first part of this two-part paper showed that those two loading techniques do not work with the RDB when testing materials with a relatively high ratio of fracture toughness to tensile strength, the square of characteristic length [3]. That paper shows that the RDB loaded in eccentric compression (Fig. 1), ASTM designation RDB(B), produces usable data for such materials. The specimen geometry is slightly different than the geometry described in ASTM E 1304. The geometry was modified so that inserts used to cast in the notch could be fastened at the tips to prevent shifting during casting of the specimen.

Data reduction for results from tests using the RDB specimen can be performed at two levels. Level I assumes linear elastic fracture mechanics (LEFM) conditions and produces the apparent fracture toughness K_{IQ} (Eq 1) where F_{max} is the maximum applied load, B and W are as shown in Fig. 1, and Y_{min}^* is the minimum normalized stress intensity factor. The minimum normalized stress intensity factor contains information about the specimen geometry, loading technique, and crack length; therefore, Y_{min}^* is a geometry calibration factor. Level II modifies the Level I result to account for nonlinear conditions and produces the size-independent fracture

toughness, K_{Ic} . Level II data reduction was developed by Barker [4] and is described in Hanson and Ingraffea [3]. This paper details the process by which Y_{min}^* has been calculated for the RDB(B) shown in Fig. 1. Two methods are used to determine Y_{min}^* : compliance calibration and direct calculation of stress intensities. Recognizing that actual test specimens will differ slightly from the geometry specified herein, the factor has been determined for an anticipated range of actual geometries.

$$K_{IQ} = \frac{Y_{min}^*}{B\sqrt{W}} \times F_{max} \quad (1)$$

What is the Normalized Stress Intensity Factor?

A unique feature of chevron-notched fracture test specimens is the way the stress intensity factor per unit load, $K_I/\text{unit load}$, changes with crack length under linear elastic fracture mechanics (LEFM) conditions (Fig. 2). The stress intensity factor per unit load initially decreases as the crack propagates. At a specific point, the stress intensity factor per unit load reaches a minimum, then begins to increase with increasing crack length. Because $K_I = K_{Ic}$ while the crack is propagating under LEFM conditions, the applied load must initially increase, then reach a maximum when $K_I/\text{unit load}$ reaches a minimum, then decrease. Consequently, under LEFM conditions, the fracture toughness can be calculated according to Eq 2, where F_{max} is the maximum applied load.

$$K_{IQ} = \left(\frac{K_I}{\text{unit load}} \right)_{min} \times F_{max} \quad (2)$$

Barker [1] showed that the point where $K_I/\text{unit load}$ reaches a minimum is practically independent of material properties. Therefore, the minimum stress intensity factor per unit load can be expressed in terms of geometry dimension values, diameter B and height W , and the minimum normalized stress intensity factor, Y_{min}^* . The expression for fracture toughness under LEFM conditions then becomes Eq 1.

Manuscript received 8/21/2001; accepted for publication 6/27/2002; published XXXXX.

¹ Visiting Assistant Professor, Bucknell University, Department of Civil and Environmental Engineering, Lewisburg, PA 17837.

² Dwight C. Baum Professor of Civil and Environmental Engineering, Cornell University, 220 Hollister Hall, Ithaca, NY 14853.

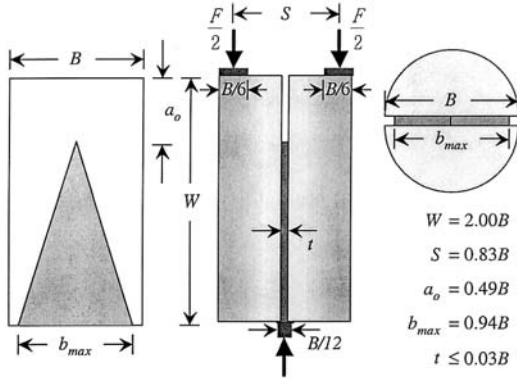


FIG. 1—The round double beam loaded in eccentric compression, RDB(B).

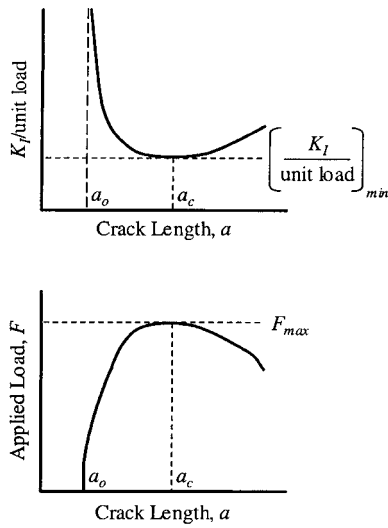


FIG. 2—Schematic of how stress intensity per unit load and applied load change with crack length in a chevron notched fracture specimen under LEFM conditions.

Compliance Calibration

Several researchers have used compliance calibration to determine the minimum normalized stress intensity factor for tension loading of various round double beam geometries [5–8]. Application of the eccentric loading technique to round double beam specimens is being first introduced in this research; therefore, no previous work has been performed to determine the minimum normalized stress intensity factor for this combination.

Compliance calibration is based upon a relationship for the energy release rate derived by Irwin and Kies [9]. The original relationship can be expressed with different symbols to obtain Eq 3. In this expression, G_I is the energy release rate, F is the applied load, b is the width of the crack front and is a function of the crack length, C is the compliance (load line displacement/load) of the specimen, and a is the crack length. For crack propagation under LEFM conditions, $G_I = G_{Ic}$, where G_{Ic} is the critical energy release rate. Using the relationship between G_{Ic} and K_{Ic} from Eq 4³, Eq 3 becomes

³ This expression is for plane strain conditions, which are typical with chevron-notched specimens (see Barker [1]). For plane stress conditions, $E/(1 - \nu^2)$ should be replaced with E . The $(1 - \nu^2)$ term is often neglected because for values of ν up to 0.3, omission causes less than 5% error in K_{Ic} .

Eq 5. Manipulation of Eq 5 results in Eq 6. This expression is correct for any specimen geometry.

$$G_I = \frac{F^2}{2b} \frac{\partial C}{\partial a} \quad (3)$$

$$G_{Ic} = \frac{K_{Ic}^2 (1 - \nu^2)}{E} \quad (4)$$

$$K_{Ic} = F \sqrt{\frac{E}{2b(1 - \nu^2)} \frac{\partial C}{\partial a}} \quad (5)$$

$$\left(\frac{K_I}{\text{unit load}} \right) = \sqrt{\frac{E}{2b(1 - \nu^2)} \frac{\partial C}{\partial a}} \quad (6)$$

The right-hand side of Eq 6 depends upon the material (E , C , and ν), the specimen size (C and a), and the specimen shape (C). Rather than determine $\partial C/\partial a$ for different materials and specimen sizes, it is typically reformulated into a nondimensional form (brackets in Eq 7). Equation 7 can be substituted into Eq 6 to obtain Eq 8. One more specimen dimension must be introduced under the radical in Eq 8 in order to make the radical nondimensional. Although any specimen dimension could be chosen, W is typically used and has been inserted to obtain Eq 9. The nondimensional portion of the right-hand side of Eq 9 is called the normalized stress intensity factor, Y^* (Eq 10).

$$\frac{\partial C}{\partial a} = \frac{1}{B^2 E} \left[\frac{\partial(CEB)}{\partial(a/B)} \right] \quad (7)$$

$$\left(\frac{K_I}{\text{unit load}} \right) = \frac{1}{B} \sqrt{\frac{1}{2b(1 - \nu^2)} \frac{\partial(CEB)}{\partial(a/B)}} \quad (8)$$

$$\left(\frac{K_I}{\text{unit load}} \right) = \frac{1}{B\sqrt{W}} \sqrt{\frac{W}{2b(1 - \nu^2)} \frac{\partial(CEB)}{\partial(a/B)}} \quad (9)$$

$$Y^* = \sqrt{\frac{W}{2b(1 - \nu^2)} \frac{\partial(CEB)}{\partial(a/B)}} \quad (10)$$

For chevron-notched specimens, the minimum normalized stress intensity factor occurs at the critical crack length, a_c (Eq 11). The critical crack length is defined as the crack length at which the crack becomes unstable under load control. This means that for any crack length larger than a_c , the stress intensity factor is increasing ($dK_I/da > 0$) for constant load. Therefore at a_c , the stress intensity factor per unit load reaches a minimum (Eq 12). Substituting Eq 11 into Eq 9 produces Eq 12.

$$Y_{\min}^* = \sqrt{\frac{W}{2b(1 - \nu^2)} \frac{\partial(CEB)}{\partial(a_c/B)}} \quad (11)$$

$$\left(\frac{K_I}{\text{unit load}} \right)_{\min} = \frac{Y_{\min}^*}{B\sqrt{W}} \quad (12)$$

The normalized stress intensity factor can be determined as a function of crack length by laboratory experiments (i.e., [6]) or through numerical simulations (i.e., [7]). This study uses numerical simulations to calculate C as a function of a in order to determine Y^* as a function of a .

The geometry and boundary conditions of the simulation models used to generate the compliance values are shown in Fig. 3. The range of model heights represents the most probable range of specimen heights that might be obtained in the laboratory. The models used in the compliance calibration study are strictly 301.5 mm

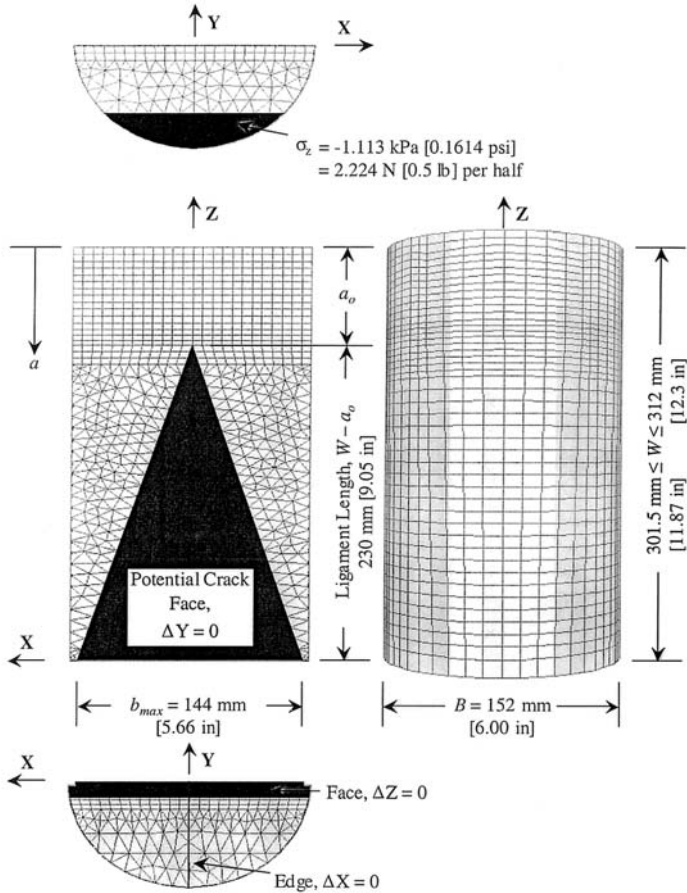


FIG. 3—Information on the RDB(B) simulation models used to generate normalized stress intensity factors.

TABLE 1—Mesh convergence study of uncracked compliance of linear elastic RDB(B) models.

Model	Degrees of Freedom	C_{avg} Values (mm/N)		
		$Y = -51$ mm	$Y = -60$ mm	$Y = -76$ mm
Compr6Ha	6,957	1.22E-6	1.51E-6	1.86E-6
Compr6Ha1	8,148	1.22E-6	1.51E-6	1.86E-6
Compr6Ha3	10,032	1.22E-6	1.51E-6	1.87E-6
Compr6Ha2	12,120	1.23E-6	1.51E-6	1.87E-6

[11.87 in.] high with a ligament length of 230 mm [9.05 in.]. The models are all three-dimensional and use the boundary element method. The linear elastic simulations were performed using the FRANC3D⁴ program.

A mesh refinement study of the compliance of the uncracked model was performed to select a basic mesh for the models. Information on the models and the compliance measured at three different locations is presented in Table 1. The derivation of Eq 3 by Irwin and Kies [9] depends on the compliance being based on the load line displacement. The RDB(B) is not loaded along a line, but

⁴ FRANC3D is written and maintained by the Cornell Fracture Group. The program is publicly available from the group's website at <http://www.cfg.cornell.edu>.

is loaded over an area. Therefore, the authors chose to calculate the normalized stress intensity factor based on compliances over the range of possible displacement measurement locations.

Each compliance value is the weighted average of displacement values in the Z-direction from points along the stated line. The displacement values were calculated at the outer edges of the specimen, points A and C in Fig. 4, and at the midpoint, point B in Fig. 4, and averaged according to Eq 13. There is only one point on the model at $Y = -76$ mm [3.0 in.]; therefore, the value along that line is not averaged.

$$C_{avg} = \frac{C_A + 2C_B + C_C}{4} \quad (13)$$

All of the meshes in Table 1 provide comparable compliance values. Therefore, the mesh of model Compr6Ha will be used to generate the compliance values for the various crack lengths. Table 2 presents the normalized compliance, *CEB*, values for the three measurement locations for a range of normalized crack lengths, a/B . The modulus of elasticity E for all of the models is 27.6 GPa [4.00E + 6 psi], and Poisson's ratio ν is 0.18. Each column of *CEB* values can be fit with a fourth-order polynomial (Figs. 5–7).

The polynomial expressions for *CEB* can be differentiated analytically and evaluated over a range of normalized crack lengths. Those values can be combined with the corresponding crack front widths b in Eq 10 to obtain normalized stress intensity factor values. The normalized stress intensity factor values Y^* are summarized in Table 3 and are plotted in Fig. 8. The minimum values are highlighted in bold.

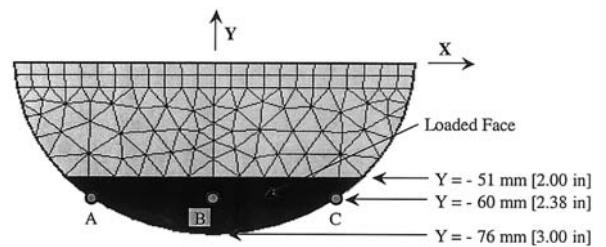


FIG. 4—Locations where compliance is measured on the RDB(B) models.

TABLE 2—Normalized compliance values as functions of normalized crack length.

Model	Norm. Crack Length, a/B	<i>CEB</i> Values		
		$Y = -51$ mm	$Y = -60$ mm	$Y = -76$ mm
Compr6Ha	0.47	5.13	6.33	7.84
Compr6Hb	0.65	5.28	6.59	8.22
Compr6Hc	0.81	5.52	6.95	8.78
Compr6He	0.98	5.78	7.35	9.40
Compr6Hf	1.06	5.93	7.57	9.73
Compr6Hw1	1.10	6.02	7.69	9.92
Compr6Hg	1.15	6.09	7.81	10.09
Compr6Hx	1.19	6.19	7.94	10.29
Compr6Hh	1.23	6.29	8.08	10.50
Compr6Hi	1.31	6.52	8.40	10.97
Compr6Hk	1.48	7.22	9.35	12.31

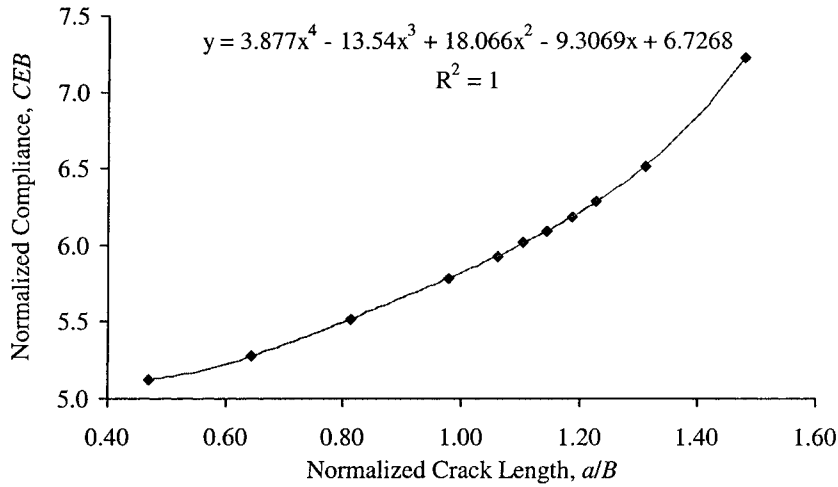


FIG. 5—Graph of normalized compliance along $Y = -51$ mm as a function of normalized crack length with the best fit fourth-order polynomial.

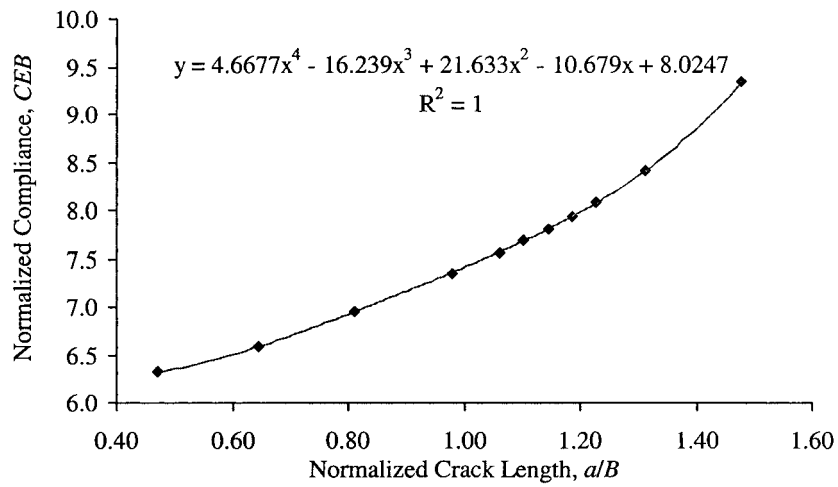


FIG. 6—Graph of normalized compliance along $Y = -60$ mm as a function of normalized crack length with the best fit fourth-order polynomial.

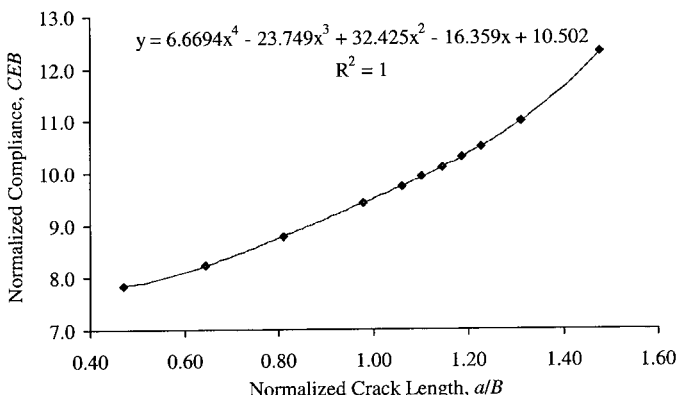


FIG. 7—Graph of normalized compliance along $Y = -76$ mm as a function of normalized crack length with the best fit fourth-order polynomial.

The values of Y_{\min}^* from Table 3 range from 2.24–3.34, and this range results from the ambiguity in where to compute C . The single value that should be used in Eq 1 lies somewhere in this range. In order to refine the estimate of Y^* the stress intensity per unit load can be calculated from simulations in which the stress intensity is evaluated directly from the local crack front displacement fields.

Direct Calculation of Stress Intensities

The stress intensity factor K_I per unit load can be calculated directly from the simulated linear elastic responses. This approach was investigated by Ingraffea et al. [7], who found reasonable agreement between the minimum normalized stress intensity factors from direct calculation and compliance calibration for an RDB(T) specimen.

TABLE 3—Normalized stress intensity factor values as functions of normalized crack length.

Norm. Crack Length, a/B	b (mm)	Y_{min}^* Values		
		$Y = -51$ mm	$Y = -60$ mm	$Y = -76$ mm
0.50	2.9	5.44	7.77	9.15
0.55	7.6	4.19	5.51	6.62
0.60	12.4	3.72	4.72	5.74
0.65	17.2	3.40	4.25	5.20
0.70	21.9	3.16	3.90	4.80
0.75	26.7	2.95	3.62	4.48
0.80	31.5	2.76	3.39	4.20
0.85	36.2	2.61	3.19	3.97
0.90	41.0	2.48	3.03	3.78
0.95	45.8	2.37	2.90	3.62
1.00	50.5	2.30	2.80	3.49
1.05	55.3	2.25	2.73	3.41
1.10	60.0	2.24	2.70	3.36
1.15	64.8	2.25	2.71	3.34
1.20	69.6	2.30	2.74	3.37
1.25	74.3	2.37	2.80	3.43
1.30	79.1	2.47	2.89	3.52
1.35	83.9	2.58	3.01	3.65
1.40	88.6	2.72	3.15	3.80
1.45	93.4	2.88	3.31	3.97
1.50	98.2	3.04	3.48	4.16

Equation 14 gives the relationship between the stress intensity factor per unit load and the normalized stress intensity factor. FRANC3D calculates stress intensity factors along the crack front using the displacement correlation method [10]. In all the simulations used here, the crack front was straight, and the average value of K_I /unit load for a particular crack length was obtained by averaging the values computed at all crack front nodes except the ends. The values at the ends were omitted due to inaccuracies in calculated displacements at edges using the boundary element method. The authors used the average K_I /unit load as the value inserted in Eq 14 to find the comparable Y^* . Therefore, the minimum normalized stress intensity factor is calculated from the smallest average K_I /unit load.

$$\left(\frac{K_I}{\text{unit load}} \right) = \frac{Y^*}{B\sqrt{W}} \tag{14}$$

The stress intensity factors calculated from the linear elastic simulations will depend upon the refinement of the boundary element mesh. To determine which models are most likely to produce the smallest average stress intensity, the stress intensities of the models described in Table 1 are compared in Table 4 and Fig. 9. The models with crack fronts at a normalized length between 1.06 and 1.23 have the lowest average stress intensities and are studied further.

The model with a normalized crack length of 1.15 was chosen for a mesh refinement study. The mesh in the region of the crack front was increasingly refined. The different models are summa-

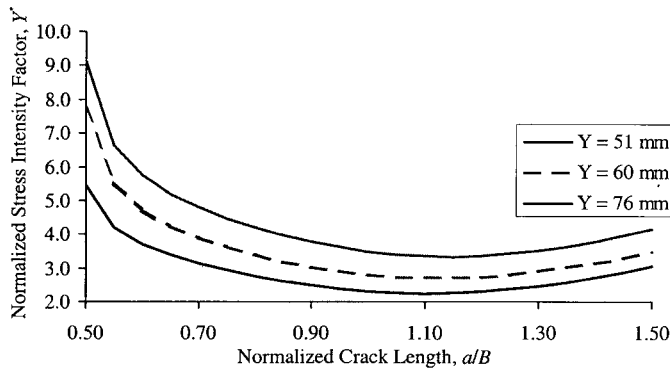


FIG. 8—Graph of normalized stress intensity factors as functions of normalized crack length.

TABLE 4—Stress intensity factor values for various crack lengths.

Model	Norm. Crack Length, a/B	K_I /unit load ($1/\text{mm}^{3/2}$)		
		Minimum	Average	Maximum
Compr6Hb	0.65	1.29E-3	1.34E-3	1.42E-3
Compr6Hc	0.81	1.01E-3	1.06E-3	1.18E-3
Compr6He	0.98	9.16E-4	9.54E-4	1.08E-3
Compr6Hf	1.06	9.12E-4	9.45E-4	1.07E-3
Compr6Hg	1.15	8.81E-4	9.11E-4	1.04E-3
Compr6Hx	1.19	8.88E-4	9.14E-4	1.04E-3
Compr6Hh	1.23	9.01E-4	9.26E-4	1.05E-3
Compr6Hi	1.31	9.45E-4	9.66E-4	1.10E-3
Compr6Hk	1.48	1.18E-3	1.20E-3	1.34E-3

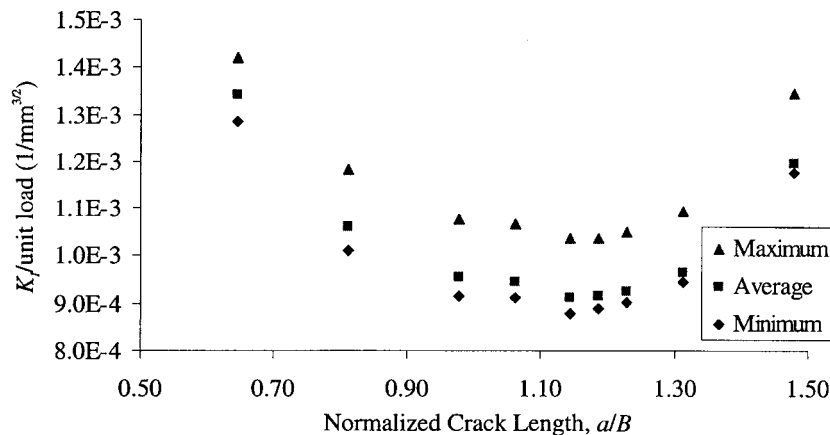


FIG. 9—Graph of stress intensity factor values for various crack lengths.

TABLE 5—Mesh convergence study of stress intensity factors for models with a normalized crack length of 1.15.

Model	Degrees of Freedom	Crack Front Elements	K_I /unit load ($1/\text{mm}^{3/2}$)		
			Minimum	Average	Maximum
Compr6Hg	7962	32	8.81E-4	9.11E-4	1.04E-3
Compr6Hg1	14094	64	8.54E-4	8.91E-4	1.10E-3
Compr6Hg2	18702	128	8.52E-4	8.93E-4	1.16E-3

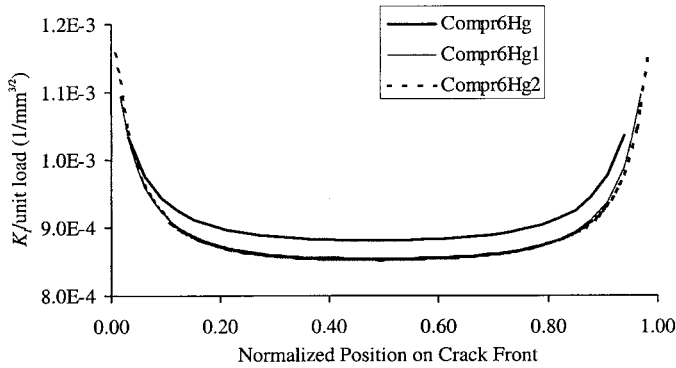


FIG. 10—Effect of mesh refinement on stress intensity factors for models with a normalized crack length of 1.15.

TABLE 6—Stress intensity factor values based on refined meshes for various crack lengths.

Model	Norm. Crack Length, a/B	K_I /unit load ($1/\text{mm}^{3/2}$)		
		Minimum	Average	Maximum
Compr6Hf1	1.06	8.90E-4	9.32E-4	1.14E-3
Compr6Hw1	1.10	8.58E-4	8.97E-4	1.10E-3
Compr6Hg1	1.15	8.54E-4	8.91E-4	1.10E-3
Compr6Hx1	1.19	8.61E-4	9.01E-4	1.14E-3
Compr6Hh1	1.23	8.74E-4	9.05E-4	1.11E-3

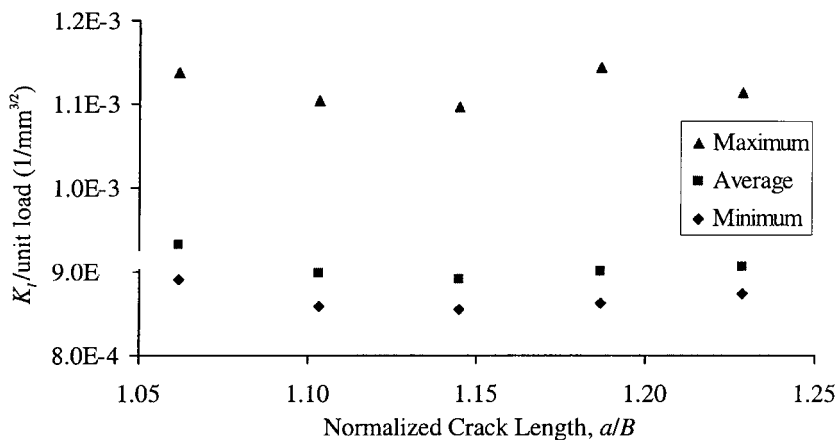


FIG. 11—Graph of stress intensity factor values based on refined meshes for various crack lengths.

rized in Table 5. The stress intensity factor values for the different models are plotted in Fig. 10. It is noteworthy that the calculated compliance values from the three models differed by less than 0.6%.

The response of the model with the most refined mesh is almost identical to the response of the intermediate mesh. For simplicity, the intermediate mesh was used with the other models with normalized crack lengths between 1.06 and 1.23. The responses of the models with different crack lengths are presented in Table 6 and Fig. 11. The minimum occurs at a normalized crack length of 1.15. The smallest average K_I /unit load is highlighted in bold. This value corresponds to a minimum normalized stress intensity factor, Y_{min}^* , of 2.357 for an RDB(B) that is 301.5 mm [11.87 in.] high. This value falls within the range expected from the compliance calibration technique.

Variations of Geometry and Loading Conditions

The minimum normalized stress intensity factor determined in the previous section pertains to an RDB(B) with set relative dimensions. When an RDB specimen is made for laboratory testing, it will almost always have slightly different relative dimensions compared to the standard geometry. Therefore, this section explores the effect of variations in relative specimen height and relative ligament height on Y_{min}^* . The model used in the previous section assumes that the pressure applied to the loaded faces is uniform. Conditions in a laboratory experiment might be different; therefore, effects of variation in pressure distribution also are investigated here.

Effect of Variations in Specimen Height

The laboratory RDB(B) specimens vary in height after they have been capped. The height of an RDB(B) specimen with a diameter of 152 mm [6.0 in.] will likely be less than 312 mm [12.3 in.]. Therefore, the smallest average K_I /unit load has been calculated for an RDB(B) that is 312 mm high. The refined meshes from the 301.5 mm [11.87 in.] high models were applied to the 312 mm high models to obtain the results in Table 7. The minimum value is highlighted in bold. This value is a small change from the 301.5 mm high model; however, Y_{min}^* becomes 2.410 for an RDB(B) that is 312 mm high.

Over this short range of specimen heights, it is assumed that Y_{\min}^* can be obtained by linear interpolation between the two calculated values. The expression for Y_{\min}^* in terms of the nondimensional ratio of specimen height W to specimen diameter B is given by Eq 15. The heights of the two models investigated translate into W/B ratios of 1.98 and 2.05.

$$Y_{\min}^* = 0.740 \times (W/B) + 0.894 \quad (15)$$

Effect of Variations in Ligament Length

For specimens that have a cut notch, the ligament length will vary, which will change Y_{\min}^* . The ligament length is given by $(W - a_o)$, where a_o is the distance from the top of the capped specimen to the tip of the triangular ligament to be cracked. Using models with an intermediate height, 310 mm [12.2 in.], the ligament length was changed to 221 mm [8.7 in.] and 236 mm [9.3 in.]. The resulting stress intensity factors are presented in Tables 8 and 9 for the respective ligament lengths. The smallest average K_I /unit load for each ligament length is highlighted in bold. These values translate to Y_{\min}^* values of 2.363 and 2.453, respectively.

TABLE 7—Stress intensity factor values based on refined meshes for an RDB(B) 312 mm high for various crack lengths.

Model	Norm. Crack Length, a/B	K_I /unit load ($1/\text{mm}^{3/2}$)		
		Minimum	Average	Maximum
Compr6Tw1	1.18	8.60E-4	8.99E-4	1.10E-3
Compr6Tg1	1.22	8.58E-4	8.95E-4	1.10E-3
Compr6Tx1	1.26	8.65E-4	8.99E-4	1.11E-3

TABLE 8—Stress intensity factor values for an RDB(B) 310 mm high with a ligament length of 221 mm.

Model	Norm. Crack Length, a/B	K_I /unit load ($1/\text{mm}^{3/2}$)		
		Minimum	Average	Maximum
Compr6TLf1	1.12	9.19E-4	9.65E-4	1.18E-3
Compr6TLg1	1.20	8.75E-4	9.14E-4	1.13E-3
Compr6TLh1	1.28	8.88E-4	9.23E-4	1.14E-3

TABLE 9—Stress intensity factor values for an RDB(B) 310 mm high with a ligament length of 236 mm.

Model	Norm. Crack Length, a/B	K_I /unit load ($1/\text{mm}^{3/2}$)		
		Minimum	Average	Maximum
Compr6THf1	1.12	8.78E-4	9.19E-4	1.12E-3
Compr6THg1	1.20	8.46E-4	8.81E-4	1.08E-3
Compr6THx1	1.24	8.54E-4	8.85E-4	1.09E-3
Compr6THh1	1.28	8.66E-4	8.95E-4	1.10E-3

The minimum normalized stress intensity factor for an RDB(B) specimen that is 310 mm high is 2.398 according to Eq 15. Therefore, by lowering the ligament length from 230 to 221 mm, the Y_{\min}^* value decreases by 2.5%. Increasing the ligament length from 230 to 236 mm causes a 2.3% increase in Y_{\min}^* . These percent changes can be represented by a calibration factor, C^* . Multiplying the Y_{\min}^* value from Eq 15 by C^* will give the minimum normalized stress intensity factor for the specimen with a cut notch. The calibration factor is given by Eq 16 where the relative ligament length is $(W - a_o)/B$.

$$C^* = 1.567 - 0.375 \times \left(\frac{W - a_o}{B} \right) \quad (16)$$

The calibration factor (Eq 16) can be combined with the minimum normalized stress intensity factor (Eq 15) to account for typical variations in geometry observed in the laboratory specimens. Therefore, the apparent fracture toughness can be calculated for laboratory test specimens using Eq 1.

Effect of Variations in Pressure Distribution on Loaded Faces

The minimum normalized stress intensity factor was derived in the previous section assuming that the load applied to the specimen is a uniform pressure. Such might not be the situation for the laboratory specimens. Therefore, the potential effect on Y_{\min}^* has been investigated. Two additional simulations based on the model producing the smallest K_I /unit load in Table 6 have been performed. The simulations have nonuniform pressure distributions on the loaded faces.

The first simulation varies the applied pressure so that it increases in going from $Y = 51$ to 76 mm [2.0 to 3.0 in.] (Fig. 12). The model is named Compr6Hg1a and has 14,121 degrees-of-freedom. The net applied load remains 4,448 N [1 lb] for the entire specimen. The stress intensity factors across the crack front are plotted in Fig. 13. The average stress intensity for the new model is 2% larger than the average value in Table 6.

The second simulation varies the applied pressure to decrease in going from $Y = 51$ to 76 mm [2.0 to 3.0 in.] (Fig. 14). The model is identical to Compr6Hg1a except for the pressure distribution. The stress intensity factors across the crack front are plotted in Fig. 15. The average stress intensity for the new model is 0.2% smaller than the average value in Table 6.

The effect of a nonuniform pressure applied to the loaded regions of the top of the RDB(B) specimen is small compared to the scatter of laboratory measurements. The situation that has the largest effect on the average stress intensity factor is increasing pressure toward the outer edge ($Y = -76$ mm) of the specimen, but the change is only 2%. Therefore, the assumption of uniform pressure on the loaded regions is reasonable. If a more detailed estimate of the pressure distribution is desired, the loading apparatus and specimen can be modeled explicitly. Such an analysis has not been conducted in this study.

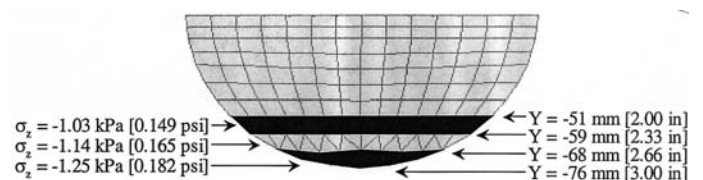


FIG. 12—Loading conditions for a model with nonuniform applied pressure.

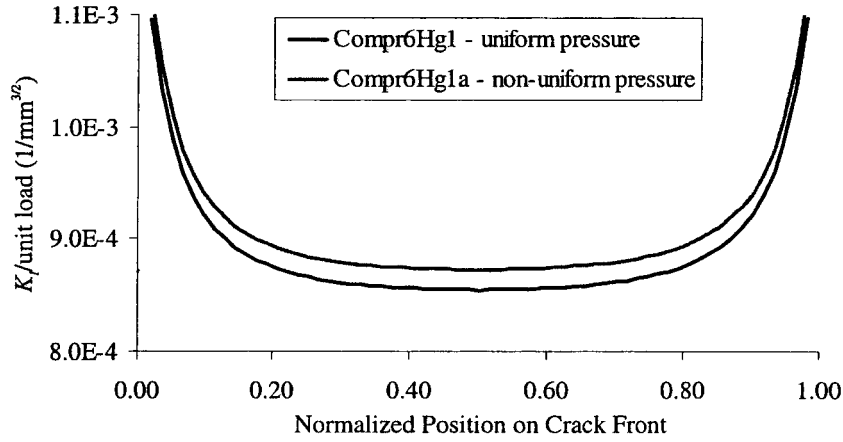


FIG. 13—Stress intensity factor values for a model with uniform and nonuniform applied pressure.

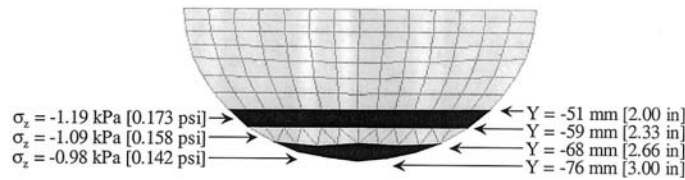


FIG. 14—Loading conditions for a model with nonuniform applied pressure.

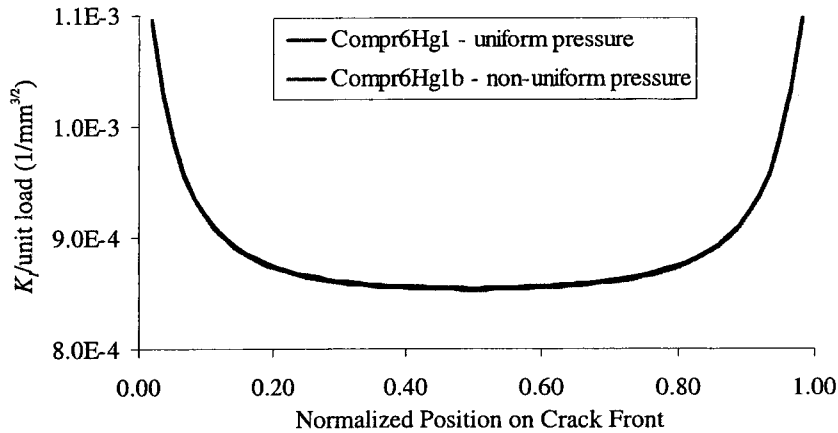


FIG. 15—Stress intensity factor values for a model with uniform and nonuniform applied pressure.

Conclusions

The round double beam specimen is an established part of several fracture toughness testing standards (ASTM B 771, ASTM E 1304, [2]). The first paper in this two part series [3] showed that the tension and wedging loading techniques used with the RDB do not produce usable results when testing materials with a relatively large characteristic length. The eccentric compression loading technique has been developed for use with RDB specimens made from such materials.

Data reduction for tests using the RDB specimen with any of the loading techniques requires the minimum normalized stress intensity factor, Y_{\min}^* . That factor depends only on the relative dimensions of the RDB geometry and the loading technique. Therefore, numerical simulations have been used to determine that Y_{\min}^* is

2.374 for the standard RDB(B) described in Fig. 1. In addition, expressions have been developed for Y_{\min}^* to account for typical variations in geometry of the laboratory specimens (Eqs 15 and 16).

Acknowledgments

This research has been made possible through grants by the National Science Foundation, Grant No. CMS-9414243, and the Alcoa Foundation. All simulations were performed in the Cornell Theory Center.

References

[1] Barker, L.M., "A Simplified Method for Measuring Plane Strain Fracture Toughness," *Engineering Fracture Mechanics*, Vol. 9, No. 2, 1977, pp. 361–369.

- [2] International Society for Rock Mechanics, "Suggested Methods for Determining the Fracture Toughness of Rock," *International Journal of Rock Mechanics and Mining Sciences & Geomechanics Abstracts*, Vol. 25, No. 2, Apr. 1988, pp. 71–96.
- [3] Hanson, J. H. and Ingraffea, A. R., "Compression Loading Applied to Round Double Beam Fracture Specimens. I: Application to Materials with Large Characteristic Lengths," *Journal of Testing and Evaluation*, Vol. 30, No. 6, pp. xxx.
- [4] Barker, L. M., "Theory for Determining K_{Ic} from Small, Non-LEFM Specimens, Supported by Experiments on Aluminum," *International Journal of Fracture*, Vol. 15, No. 6, Dec. 1979, pp. 515–536.
- [5] Barker, L. M., "Compliance Calibration of a Family of Short Rod and Short Bar Fracture Toughness Specimens," *Engineering Fracture Mechanics*, Vol. 17, No. 4, 1983, pp. 289–312.
- [6] Bubsey, R. T., Munz, D., Pierce, W. S., and Shannon, J. L., Jr., "Compliance Calibration of the Short Rod Chevron-Notch Specimen for Fracture Toughness Testing of Brittle Materials," *International Journal of Fracture*, Vol. 18, No. 2, Feb. 1982, pp. 125–133.
- [7] Ingraffea, A. R., Gunsallus, K. L., Beech, J. F. and Nelson, P. P., "A Short-Rod Based System for Fracture Toughness Testing of Rock," *Chevron-Notched Specimens: Testing and Stress Analysis*, ASTM STP 855, J. H. Underwood, S. W. Freiman, and F. I. Baratta, Eds., ASTM International, West Conshohocken, PA, 1984, pp. 152–166.
- [8] Shannon, J. L. Jr., Bubsey, R. T., Pierce, W. S., and Munz, D., "Extended Range Stress Intensity Factor Expressions for Chevron-Notched Short Bar and Short Rod Fracture Toughness Specimens," *International Journal of Fracture*, Vol. 19, No. 3, July 1982, pp. R55–R58.
- [9] Irwin, G. R. and Kies, J. A., "Critical Energy Rate Analysis of Fracture Strength," *Welding Journal*, Welding Research Supplement, American Welding Society, Miami, FL, Vol. 32, 1954, pp. 193–198.
- [10] Chan, S. K., Tuba, I. S., and Wilson, W. K., "On the Finite Element Method in Linear Fracture Mechanics," *Engineering Fracture Mechanics*, Vol. 2, No. 1, July 1970, pp. 1–17.